Electron Scattering and Electrical Conductance in Polycrystalline Metallic Films and Wires: Impact of Grain Boundary Scattering Related to Melting Point

Y. F. Zhu, X. Y. Lang, W. T. Zheng, and Q. Jiang*

Key Laboratory of Automobile Materials (Jilin University), Ministry of Education, and School of Materials Science and Engineering, Jilin University, Changchun 130022, China

ABSTRACT For electrical conductance in polycrystalline metallic films and wires, the reflection coefficient of electrons at grain boundaries is explored and found to be proportional to the square root of the melting points of metals. As validated by available experimental results, this exploration enables classical models to take an essential role in theoretically predicting the electrical conductance of low-dimensional metals. One thus sees that the mechanism dominating the suppression of electrical conductance is transformed from the surface scattering into the grain boundary scattering as the ratio of film thickness (or wire diameter) to grain size rises. Furthermore, the impact of grain boundary scattering becomes less important for metals with lower melting points.

KEYWORDS: electrical conductance · grain boundary scattering · surface scattering · polycrystalline · films · wires

Polycrystalline metallic films and wires have important applications in microelectronics, such as ultralarge scale integration, thermoelectric power generation, and magnetic data storage.[1−4] As the film thickness or wire diameter D and/or the grain size L approaches the length scale of the electron mean free path $l(T,\infty,\infty)$, the corresponding electrical conductivities $\sigma(T,D,L)$ deviate downward from their bulk values $\sigma(T,\infty,\infty)$,[5,6] where ∞ denotes the bulk size and T denotes the Kelvin temperature. This deviation is induced by the surface scattering (SS) and/or the grain boundary scattering (GBS) especially when D and/or L are much smaller than $l(T,\infty,\infty)$ at low T,[1,7] which is a fundamental obstacle for high speed electronic applications with polycrystalline films and wires. Although there have been ample discussions about the correlation between scattering mechanisms and electrical conductance,[5,6,8−11] present theoretical models for predicting $\sigma(T,D,L)$ functions still require further development for perfection.

The SS effect on $\sigma(T,D,L)$ of single crystalline films and wires was first considered rigorously by Fuchs and Sondheimer (FS model) in the 1930s−1950s with the classical Boltzmann equation based on the free electron theory,[5,8,11] which is conveniently denoted with $\sigma_s(T,D)$ by omitting the parameter L where $L \rightarrow \infty$. In the FS model, assuming that the Fermi velocity surface is spherical, the distribution function of the conduction electrons is constructed as a function of the position and velocity vectors. Given that the specularity parameter is a constant that is independent of the motion direction of electrons, introducing polar coordinates in the velocity vector space, $\sigma_s(T,D)$ was derived.[5,11] The specularity parameter here means the fraction of electrons that are scattered elastically at both the surface and the film/substrate interface. Since this parameter cannot be measured directly, it is usually used as an adjustable parameter ranging from zero to unity depending on the physical nature of atomic arrangement at the surface and interface.[12,13] For nonepitaxially grown polycrystalline metallic films or wires, the electron scattering should be diffusive,[12−15] which leads the specularity parameter to being equal to zero. An important reason for this is attributed to the lattice contraction at surfaces[16] and the nonepitaxial relation at film/substrate interfaces. In this simple case, $\sigma_s(T,D)/\sigma(T,\infty,\infty) = 1 - 3k\int_1^\infty(x^{-3} - x^{-5})(1 - e^{-x/k})\,dx/2$ for films, and $\sigma_s(T,D)/\sigma(T,\infty,\infty) = 1 - (12/\pi)\int_0^1(1 - x^2)^{1/2}[\int_1^\infty e^{-xt/k}(t^2 - 1)^{1/2}t^{-4}\,dt]dx$ for wires, where $k = l(T,\infty,\infty)/D$.[5,11]

*Address correspondence to jiangq@jlu.edu.cn.

Received for review February 10, 2010 and accepted June 9, 2010.

Published online June 17, 2010.
10.1021/nn101014k

© 2010 American Chemical Society

In the 1960s, Parrott,[17] Brändli,[18] and Soffer[9] attempted to reformulate the above FS model by using a specularity parameter as the function of the collision angle of electrons. These works played an important role in enhancing our understanding on the SS mechanism. However, additional parameters related to surface conditions, such as the root-mean-square roughness,[9] surface asperities,[17] and/or the cutoff angle,[18] are needed. Since these quantities are case-dependent and difficult to be measured experimentally, the modified FS models cannot be adopted directly for evaluating the SS effect yet. Considering that the specularity parameter equaling zero in the FS model has been demonstrated as reasonable for polycrystalline films and wires without big error,[12−15] the resultant $\sigma_s(T,D)$ equation[5,11] shown above will be adopted in this work.

In 1970s, a well-known model was established by Mayadas and Shatzkes (MS model) to elucidate the GBS effect on σ for more general cases of polycrystalline films or wires, denoted as $\sigma_g(T,L)$ by omitting D for the case of $D \gg L$.[6] According to the MS model, electrons transmitted through grain boundaries are subjected to the scattering from the gain boundary potentials, in the form of a delta-function randomly distributed throughout the polycrystalline film. If the electron reflection coefficient at grain boundaries is isotropic, $\sigma_g(T,L)$ could then be expressed as[6]

$$\sigma_g(T,L)/\sigma(T,\infty,\infty) = 3[1/3 - \alpha/2 + \alpha^2 - \alpha^3 \ln(1 + 1/\alpha)] \quad (1)$$

where $\alpha = l(T,\infty,\infty)R/[L(1-R)]$. R here refers to the probability for a conduction electron to be elastically reflected upon striking at each grain boundary ($0 < R < 1$). $\sigma_g(T,L) \rightarrow \sigma(T,\infty,\infty)$ when $R \rightarrow 0$, whereas $\sigma_g(T,L) \rightarrow 0$ when $R \rightarrow 1$.

Similar to Soffer's and other researcher's studies on $\sigma_s(T,D)$,[9,18,17] an investigation has been made by Knäbchen[19] to model $\sigma_g(T,L)$ based on a detailed analysis of the evolving residual-resistivity dipole surrounding planar defects, which relies on the incidence angle of electrons there. This work makes the GBS effect more comprehensive. However, it remains incomplete since R as the function of the incidence angle was not established effectively, probably related to the complicated defect nature at grain boundaries. Instead, the above MS model with a constant R itself[6] is simple and has been widely adopted. Since we pursue a more simple equation with easy usability, the simple MS model will be used for assessing the GBS effect in this work.

Considering that both the SS and GBS effects may take place in real films and wires especially when the sizes of D and L of the films and wires are comparable, $\sigma(T,D,L)$ of polycrystalline films and wires must come from the both contributions. To elucidate it, the both effects should be combined into one equation, which guarantees that we can later compare our results with experimental evidence. The best mathematical solution for this case is the Mathiessen's rule. Thus, we unite the above two models into one expression as follows,

$$\sigma(T,D,L)^{-1} = \sigma_g(T,L)^{-1} + \sigma_s(T,D)^{-1} - \sigma(T,\infty,\infty)^{-1} \quad (2)$$

The net variances in the $\sigma(T,D,L)^{-1}$, $\sigma_s(T,D)^{-1}$, or $\sigma_g(T,L)^{-1}$ thus follow immediately as $\Delta\sigma(T,D,L)^{-1} = \Delta\sigma_s(T,D)^{-1} + \Delta\sigma_g(T,L)^{-1}$ with $\Delta\sigma_s(T,D)^{-1} = \sigma_s(T,D)^{-1} - \sigma(T,\infty,\infty)^{-1}$ and $\Delta\sigma_g(T,L)^{-1} = \sigma_g(T,L)^{-1} - \sigma(T,\infty,\infty)^{-1}$.

To determine $\sigma_g(T,L)$ or $\sigma(T,D,L)$ using eq 1 or 2, it is required to predetermine the reflection coefficient R. On the basis of the quantum theory[20] for electrons in metals with $E_{0g} < U_g$, where E_0 denotes kinetic energy, U is the potential height, and the subscript g denotes the grain boundaries, 1-R is essentially the tunneling probability through a barrier of width ξ and height U_g,[21] which reads

$$R = 1 - \{1 + U_g^2 \sinh^2[\xi\sqrt{2m(U_g - E_{0g})}/\hbar]/[4E_{0g}(U_g - E_{0g})]\}^{-1} \quad (3)$$

where $\hbar = 1.054 \times 10^{-34}$ J·s is the Planck constant and $m = 9.108 \times 10^{-31}$ kg is the electron mass. Hence by knowing ξ, U_g, and E_{0g}, R could then be determined. In the present study, we assumed $\xi = h/3$, using a grain boundary model represented by a two-dimensional boundary structure between two hard-spheres,[16,22] where h denotes the bond length. However, the other two parameters of U_g and E_{0g} for metals are yet to be determined at this stage, impeding a theoretical evaluation of R.

Alternatively, R can be obtained by fitting the experimental $\sigma_g(T,L)$ or $\sigma(T,D,L)$ results in terms of eq 1 or 2.[10,14,15] With this method, however, although these equations may help us understand experimental results physically, it is case-dependent and cannot lead to solid foundations for further theoretical predictions. This is especially true when the R values vary considerably for the same metal among literatures, as collected in Figure 1. For example, R ranged from 0.24 to 0.80 for Cu[6,14,23] and from 0.15 to 0.7−0.9 for Au.[24,30] Such discrepancies might be due to the complicity in the $\sigma_g(T,L)$ or $\sigma(T,D,L)$ function. The SS effect is evident especially when $D < 10$ nm[6,25] owing to the perfectly diffusive scattering at both the surface and the film/substrate interface.[12,14,15] In some studies,[26−28,34] if such effect is not considered adequately on the assumption of partially or even fully specular reflection of electron scattering, R will be raised substantially using the specularity parameter higher than zero or even up to unity. Similarly, the presence of impurities and/or discontinuities drops $\sigma(T,D,L)$ and thus increases R.[14,23] Experimental errors in measuring L or σ may also lead to large inconsistencies in R where a downward deviation of L and/or an upward deviation of σ relative to the actual values result in lower R values. In particular, the precise mea-

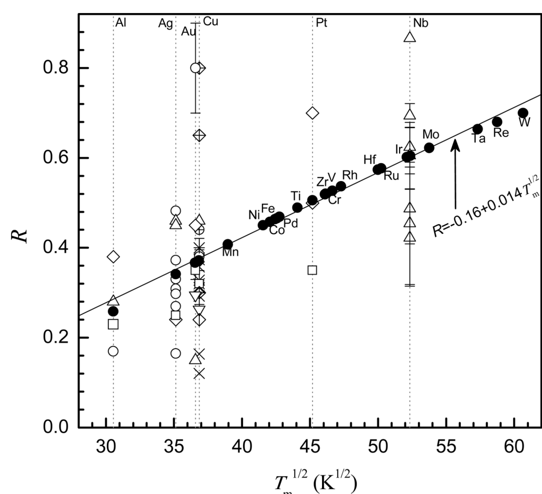

Figure 1. R as the function of $T_m^{1/2}$ in light of eq 4 given by the solid symbol (●) for selected metals, where the solid line comes from $R = -0.16 + 0.014T_m^{1/2}$. Other symbols show the reported fitting results of R using measured $\sigma(T,D,L)$ for Al,[6,65,66] Ag,[34,52,66] Au,[24,25,30,31,48] Cu,[3,4,6,14,15,23,27,28,67−70] Pt,[61,71] and Nb.[27] T_m of metals are cited from ref 37.

surement of L is very difficult since it varies widely over the whole grown films and wires,[29] while the averaged L values detected with the more convenient technique of X-ray diffraction are usually smaller than those detected with transmission electron microscopy.[14,15,29,28] Note that distinct measurement techniques may also give different results of R. As shown by Au films, R = 0.7−0.9 measured by the scanning tunneling potentiometry[24] is much larger than those obtained by the fitting technique using measured $\sigma(T,D,L)$ values in light of eq 2.[25,30,31] These scattered results lead to diffiulty in judging which R should be suitable for evaluating $\sigma_g(T,L)$ or $\sigma(T,D,L)$ and to arguments of how GBS or SS would affect $\sigma(T,D,L)$ of polycrystalline films or wires on varying D and/or L.[3,32−34] Moreover, the material-dependence of R also remains unclear, which hinders our understanding of the defect-induced variation of $\sigma_g(T,L)$ or $\sigma(T,D,L)$.

To address the above-mentioned issues, a theoretical prediction of R of polycrystalline metallic films and wires was developed, and the relative effects of GBS and SS on $\sigma(T,D,L)$ are discussed quantitatively. Equation 2 with our modeled R indeed reproduces experimental results of $\sigma(T,D,L)$, which suggests that this equation can be utilized for the theoretical prediction of $\sigma(T,D,L)$ function. Such a result will also be potentially useful for designing the microelectronic devices.

MODEL

In the present theory, the unknown parameters of U_g and E_{0g} in eq 3 will be determined from the quantum mechanics and thermodynamics ways. The results will be further simplified by eliminating the complicated hyperbolic function.

We first consider the well-studied surface properties of metals, such as E_{0s}, U_s, the work function Φ_s, the Fermi energy E_{Fs}, and the surface energy γ_s.[35−39] Since $U_s \propto \Phi_s$[35] and $\Phi_s \propto \gamma_s$,[39,40] it reads $U_s \propto \gamma_s$. In light of $E_{Fs} = U_s - \Phi_s$ and $E_{0s} = 3E_{Fs}/5$,[35] one thus gets $E_{0s} = 3(U_s - \Phi_s)/5$ or $E_{0s} \propto \gamma_s$. As a result, $U_s \propto E_{0s} \propto \gamma_s$. If this relationship is also valid for grain boundaries, $U_g \propto E_{0\,g} \propto \gamma_g$ and thus $U_g/U_s = E_{0g}/E_{0s} = \gamma_g/\gamma_s$, where γ_g denotes the grain boundary energy. Substituting it into eq 3 with aforementioned $\xi = h/3$, $R = 1 - \{1 + U_s^2 \sinh^2[h(2m(U_s - E_{0s})\gamma_g/\gamma_s)^{1/2}/(3\hbar)]/ [4E_{0s}(U_s - E_{0s})]\}^{-1}$. For some selected elements in Table 1, $E_{0s}/U_s \approx 2/5$. Thus, $U_s^2/[4E_{0s}(U_s - E_{0s})] = 25/24 \approx 1$ or $R \approx 1-\{1+\sinh^2[h(6mU_s\gamma_g/(5\gamma_s))^{1/2}/(3\hbar)]\}^{-1}$. Since $(U_s/\gamma_s)^{1/2} \approx 1.0 \times 10^{-9}$ m for metals in Table 1, $R \approx 1 - \{1+\sinh^2[10^{-9}h(6m\gamma_g/5)^{1/2}/(3\hbar)]\}^{-1}$. Considering that γ_g is about twice of the solid−liquid interface energy with regards to h, the vibrational entropy S_{vib}, the melting entropy S_m, and the melting point T_m,[37] one has $\gamma_g = 4T_mS_{vib}S_mh/(3VR_0)$,[37] where $V = N_A\pi h^3/6$ is the molar volume, R_0 = 8.314 J mol^{-1} K^{-1} is the gas constant, and $N_A = 6.02 \times 10^{23}$ mol^{-1} is the Avogadro constant. Since $S_{vib}S_m \approx R_0^2$ for metals,[37,41] a more simple γ_g expression can be shown with $\gamma_g = 8hR_0T_m/(\pi N_Ah^2)$, which provides us a convenient way to solve R in an analytical form with two material constants h and T_m. Since h can be eliminated by inserting this γ_g relation into the above R equation, only the amount T_m remains. Combining the constants $\hbar$, m, R_0, π, and N_A into the precoefficient, one gets $R \approx [1+ \sinh^{-2}(\sqrt{T_m}/50)]^{-1}$. By omitting the negligible term $\exp(-\sqrt{T_m}/25)$, R is readily read as

$$R = 1 - 4/[\exp(\sqrt{T_m}/25) + 2]. \quad (4)$$

In light of eq 4, R can be calculated with a unique well-known parameter T_m. Note that since T_m is a weak function of L,[16,37] its size dependence is therefore neglected as the first order approximation.

RESULTS AND DISCUSSION

Figure 1 shows R as the function of $T_m^{1/2}$ in light of eq 4 for the most useful metals as electric conductors. R increases with $T_m^{1/2}$ from 0.26 for Al with the lowest T_m to 0.70 for W with the highest one. Interestingly, R is almost a linear function of $T_m^{1/2}$. With the fitting technique, we have $R = -0.16 + 0.014T_m^{1/2}$. Since T_m is proportional to its cohesive energy or U_g,[37] R is essentially related to the bond strength or the crystalline stability of metals. Namely, stronger bond strength leads to larger scattering on grain boundaries. Although the reported R values for Al, Ag, Au, Cu, Pt, and Nb films or wires shown in Figure 1 vary considerably as aforementioned, these values were almost distributed evenly on both sides of our predicted values or the curve. The upward or downward deviation of reported values from our predictions should be attributed to the reasons described above.

TABLE 1. Parameters of γ_s, U_s, Φ_s, E_{Fs}, and E_{0s} Used for the Calculation of R

	γ_s[37] (J/m²)	U_s ($\times10^{-18}$J)[a]	Φ_s[49] ($\times10^{-18}$J)	E_{Fs}[50] ($\times10^{-18}$J)	E_{0s} ($\times10^{-18}$J)[b]	E_{0s}/U_s	$(U_s/\gamma_s)^{1/2}$ ($\times10^{-9}$m)
Ag	1.37	1.39	0.51	0.88	0.53	0.38	1.01
Al	1.65	2.10	0.68	1.42	0.85	0.41	1.13
Au	1.50	1.40	0.51	0.89	0.53	0.38	0.97
Co	2.52	2.80	0.92	1.88	1.13	0.40	1.05
Cr	2.91	2.51	0.74	1.77	1.06	0.42	0.93
Cu	1.79	1.67	0.53	1.13	0.68	0.41	0.96
Fe	2.42	2.53	0.75	1.78	1.07	0.42	1.02
Hf	2.46	1.87	0.71	1.16	0.70	0.37	0.87
Ir	3.45	2.68	1.10	1.58	0.95	0.35	0.88
Mn	1.97	2.45	0.70	1.75	1.05	0.43	1.11
Mo	2.90	2.75	0.82	1.94	1.16	0.42	0.97
Nb	2.68	2.52	0.75	1.77	1.06	0.42	0.97
Ni	2.38	2.81	0.92	1.88	1.13	0.40	1.09
Pd	2.12	2.36	0.81	1.54	0.93	0.39	1.05
Pt	2.92	2.87	0.89	1.99	1.19	0.41	0.99
Re	3.60	3.57	0.94	2.63	1.58	0.44	1.00
Rh	3.09	2.58	0.97	1.61	0.97	0.38	0.91
Ru	3.04	2.54	0.93	1.62	0.97	0.38	0.91
Ta	2.90	2.54	0.78	1.76	1.06	0.42	0.94
Ti	2.15	2.11	0.74	1.37	0.82	0.39	0.99
V	2.59	2.36	0.80	1.55	0.93	0.40	0.95
W	3.27	2.74	0.82	1.93	1.16	0.42	0.92
Zr	2.31	1.82	0.68	1.14	0.68	0.38	0.89

[a] $U_s = \Phi_s + E_{Fs}$. [b] $E_{0s} = 3E_{Fs}/5$.

Figure 2 shows $\sigma_g(T,L)$ as the function of L in light of eq 1 using our predicted R values for nanostructured (NS) Cu at $T = 4.2$ and 298 K (Figure 2a,b), NS Au at $T = 4.2$ K (Figure 2c) and NS Ni at $T = 77$ K (Figure 2d) where $L \ll D$ and only the GBS effect dominates $\sigma(T,D,L)$ functions or $\sigma(T,D,L) \approx \sigma_g(T,L)$. The cases with the maximal and minimal R values among those reported for NS Cu[6,14,23] and NS Au[8,24,30] were also typically plotted for comparison. Our predicted curves correspond roughly to available experimental results, while the cases with reported R values differ from those measured values. This suggests that R from eq 4 is suitable for predicting the GBS impact. Note that the experimental data of NS Au at $D = 76$ nm deviate significantly from our prediction, which might be related to errors in measurement of σ or L as mentioned above.

With our predicted R values from eq 4, $\sigma(T,D,L)$ as a function of D is shown in Figure 3 for Cu, Au, Al, Ag, Pt, and Nb films and/or wires based on eq 2. Since L is comparable to D, impacts of both GBS and SS arise. Studies[42,43] have shown that L in polycrystalline films or wires rises with increasing D driven primarily by boundary-curvature forces during the fabrication, which is greatly influenced by the fabrication tech-

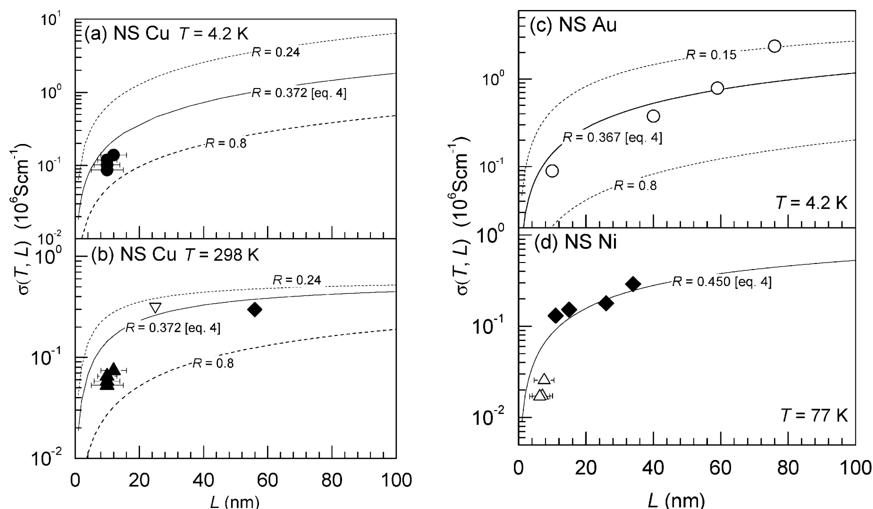

Figure 2. $\sigma_g(T,L)$ **as a function of** L **for NS Cu at (a)** $T = 4.2$ **K and (b)** $T = 298$ **K; (c) NS Au at** $T = 4.2$ **K and (d) NS Ni at** $T = 77$ **K in light of eq 1 (solid line) with our predicted** R **values from Figure 1. The cases with the maximal and minimal** R **values among those reported for Cu[6,14,23] and Au[24,30] (dashed lines) are also plotted for comparison. The symbols denote the measured results for Cu,[28,72] Au,[73,74] and Ni.[60,75] See Table 2 for other necessary parameters.**

TABLE 2. Parameters Necessary for Calculation with L as the Function of D Reported for Films and Wires

	T (K)	$\sigma(T,\infty,\infty)$ (10^6 S cm^{-1})	$l(T,\infty,\infty)^a$ (nm)	L as the function of D of films or wires^b
Ag	298	0.63[55]	53.2	films: $L = 200$ nm with 32 nm $< D <$ 780 nm;[51] $L = cD$ with $c = 0.2$[52] and 1;[34] $L = 8.44617 + 0.32122D + 0.00177D^2$ [26]
Al	4.2	91[6]	7500	films: $L = cD$ with $c = 0.2$[52] and 1[6,65]
	323	0.23[65]	19.2	
Au	4.2	6.67[48]	600	films: $L = cD$ with $c = 0.2$,[52] 1,[31] 2.2, 2.3, 3.0 and 3.3;[48] $L = 13.3 \times (1 - 0.62384^D)$.[53]
	298	0.426[55]	41	Wires: $L = 20$, 40,[8] or 80 nm[54] for any D
Cu	4.2	500[3]	33000	films: $L = -39.2 + 2.6D$;[3] 20 nm $< L <$ 48 nm with $D = 100$ nm;[67] $L = cD$ with $c = 0.167$ and 0.435,[14] 0.6,[28] 1,[76] 1.02, 1.11 and 1.12,[68] 1.2 and 1.5;[69]
	298	0.59[14]	39	$L = 137.9 - 141.3 \times 0.99408^D$;[27] $L = 6.4 + 0.45D$.[56] Wires: $L = -91.6 + 1.64D$ with 70 nm $< D <$ 240 nm and $L = 430$ nm with 70 nm $< D <$ 240 nm;[57] $L = 125$ nm;[58] $L = 25$ nm;[58] $L = -130.1 + 2.15D$;[46] $L = 17.7 + 9.61e^{(D+69.3)/97.5}$ [59]
Nb	298	0.066[27]	5.7[27]	films: $L = 21.587 - 19.71 \times 0.97988^D$ [27]
Ni	77	1.33[60]	136	
Pt	298	0.094[61]	18.5	films: $L = 0.4D$;[61] $L = 17.8 \times (1 - e^{-0.25611D})$[53]

^{a}Except Nb, the values of $l(T,\infty,\infty)$ for other metals are given in light of $l(T,\infty,\infty)/\sigma(T,\infty,\infty) = p$ where $p = 8.2 \times 10^{-6}$ $\mu\Omega$ cm^2 for Al,[6] 8.4×10^{-6} $\mu\Omega$ cm^2 for Ag,[62] 9.0×10^{-6} $\mu\Omega$ cm^2 for Au,[25] 6.6×10^{-6} $\mu\Omega$ cm^2 for Cu,[6] 10.2×10^{-6} $\mu\Omega$ cm^2 for Ni,[55,63] and 19.7×10^{-6} $\mu\Omega$ cm^2 for Pt.[64] ^{b}For interconnection wires with rectangle cross-section with the width w and the depth t, if $w \ll l(T,\infty,\infty)$ and $t \ll l(T,\infty,\infty)$ is met, the electron scattering will be much more serious at the surface and side walls. For convenience, the interconnection wires are treated as circular wires with $D = 2wt/(w + t)$ in light of the equivalent surface/volume ratio.[5]

niques and conditions. As a result, L is a scattered function of D,[44−46] as summarized in Table 2. Thereby, a median value of D for L is taken for the calculation in Figure 3a−f. As shown in Figure 3, $\sigma(T,D,L)$ decreases with reducing D for both wires and films due to enhanced scatterings at surfaces and grain boundaries. Our prediction curves go through the available experimental results denoted by symbols, supporting the validity of our predicted R values. In addition, the distinction in $\sigma(T,D,L)$ between films and wires at the same D in Figure 3 should be attributed to relative contributions from the SS and GBS effects. Relative to that of films, the $\sigma(T,D,L)$ of wires are low at $T = 4.2$ K for Cu in Figure 3a and at $T = 298$ K for Au in Figure 3b. The former is basically attributed to the relatively large decrement in $\sigma_s(T,D)$ of Cu wires induced by its serious SS effect related to high surface/volume ratio A/V, although the GBS impact is small since L of wires and films are comparable. In fact, the somewhat increasing $l(T,D)$ with $l(T,\infty,\infty)$ at low T for films[5] would push its $\sigma(T,D,L)$ curve upward, contributing also to their distinction. Similarly, the latter is also principally contributed from the serious SS impact of Cu wires. Besides it, further downward move of $\sigma(T,D,L)$ of wires caused by its high GBS impact enlarges their difference, since $L = 40$ nm for wires is lower than that of films at $D > 20$ nm or so. Noticeably, the discrepancy between wires and films is found negligible for Cu at $T = 298$ K in Figure 3a. In this case, the distinction induced by the SS effect is much shortened by the downward move of $\sigma(T,D,L)$ for films owing to its strong GBS impact, since L of films is small relative to that of wires.

With our predicted R values, we can now discuss the lone contribution of GBS or SS on the $\sigma(T,D,L)$ func-

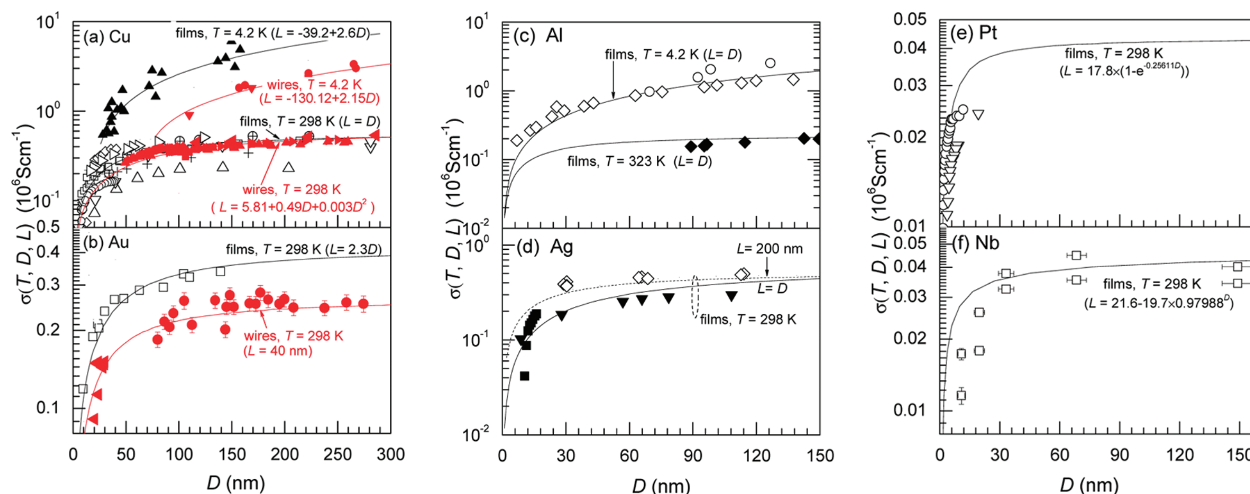

Figure 3. The $\sigma(T,D,L)$ curves as a function of D in terms of eq 2 for polycrystalline films (solid) or wires (solid and red) at $T = 4.2$, 298, or 323 K with our predicted R values from Figure 1, where a median function of D for L for calculation is given based on Table 1. The symbols denote the experimental results for Cu films at $T = 4.2$ K[3] and 298 K,[15,27,56,68,28,76] Cu wires at $T = 4.2$ K[45,46,77] and 298 K (red),[46,57,77−79] Au films[31] and Au wires (red)[54,80] at $T = 298$ K, Al films at $T = 4.2$ K[6,52] and 323 K,[65] Ag,[34,51,26] Pt,[53,61] and Nb films[27] at $T = 298$ K. See Table 2 for other necessary parameters.

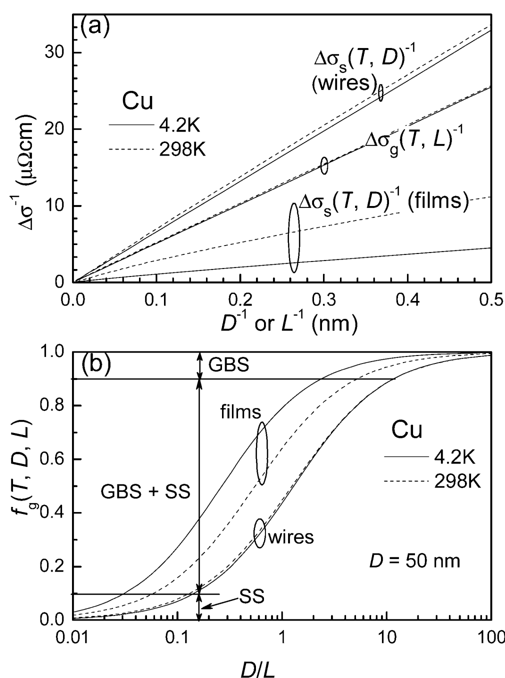

Figure 4. (a) $\Delta\sigma_g(T,L)^{-1}$ and $\Delta\sigma_s(T,D)^{-1}$ as the function of D^{-1} or L^{-1} for Cu films and wires at $T = 4.2$ and 298 K with our predicted R values from Figure 1. (b) $f_g(T,D,L) = \Delta\sigma_g(T,L)^{-1}/\Delta\sigma(T,D,L)^{-1}$ as the function of D/L at a given $L = 50$ nm with our predicted R values from Figure 1. See Table 2 for other necessary parameters.

tion by investigating their net decrements $\Delta\sigma_g(T,L)^{-1}$ and $\Delta\sigma_s(T,D)^{-1}$ defined above with the example of Cu. As plotted in Figure 4a, the amount of $\Delta\sigma^{-1}$ increases upon raising L^{-1} or D^{-1}. $\Delta\sigma_g(T,L)^{-1}$ at $T = 4.2$ K is almost the same as that at $T = 298$ K, as is $\Delta\sigma_s(T,D)^{-1}$ for wires. In comparison with $\Delta\sigma_s(T,D)^{-1}$ of wires, $\Delta\sigma_s(T,D)^{-1}$ of films is low, while $\Delta\sigma_s(T,D)^{-1}$ of films at $T = 4.2$ K is interestingly low relative to $T = 298$ K. The D- and T-dependent distinctions in $\Delta\sigma_s(T,D)^{-1}$ between wires and films are illustrated as follows.

At high T where $l(T,\infty,\infty)$ is small, the conduction electrons in the region close to the surface of the films or wires only are diffusively scattered. As a result, $l(T,D)$ drops slightly,[5,8] and the deviation in the current density from the bulk case under the same applied field is appreciable merely in the region close to the surface. $\Delta\sigma_s(T,D)^{-1}$ is thus proportional to $A/V \propto 1/D$ for both films and wires.[5,8] Since the A/V ratio of films is smaller than that of wires at the same D, $\Delta\sigma_s(T,D)^{-1}$ of films is therefore lower than that of wires in Figure 4a.

On the other hand, at low T with large $l(T,\infty,\infty)$, the conduction electrons over the cross-section are scattered more severely at the surfaces. Since $l(T,D)$ for films is still somewhat enlarging continuously,[5,8] $\Delta\sigma_s(T,D)^{-1}$ of films at $T = 4.2$ K becomes low relative to $T = 298$ K [Figure 4a]. As for wires, however, considering that $l(T,D)$ is limited to D with $\Delta\sigma_s(T,D)^{-1} \propto 1/D$,[47] being similar to the case at high T, the variation in $\Delta\sigma_s(T,D)^{-1}$ can thus hardly be observed between 4.2 and 298 K [Figure 4a].

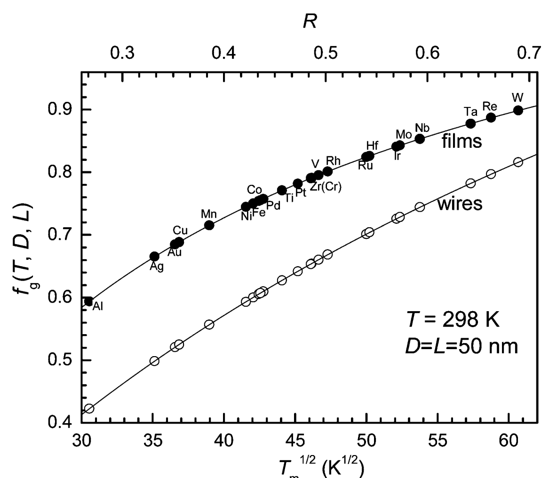

Figure 5. $f_g(T,D,L)$ as the function of R or $T_m^{1/2}$ for polycrystalline films and wires of selected metals at a given $T = 298$ K and $D = L = 50$ nm with our predicted R values from eq 4, where $f_g(T,D,L) = 2R/(1+R)$ for wires, and $f_g(T,D,L) = 4R/(1 + 3R)$ for films.

The impact of GBS is also evaluated for clarity by plotting $f_g(T,D,L) = \Delta\sigma_g(T,L)^{-1}/\Delta\sigma(T,D,L)^{-1}$ as a function of D/L for films and wires in Figure 4b with a given $D = 50$ nm. $f_g(T,D,L)$ increases for each from 0 to 1 as the D/L is raised, indicating that the mechanism dominating the suppression of $\sigma(T,D,L)$ is transformed from SS into GBS. Moreover, $f_g(T,D,L)$ is almost T-independent for wires but T-dependent for films, and the impact of GBS is high for films relative to that of wires especially at $T = 4.2$ K. In the limiting case, the SS effect dominates at $f_g(T,D,L) \to 0$ when $D/L < 0.1$ at $T = 4.2$ and 298 K for wires, and when $D/L < 0.05$ at $T = 298$ K and $D/L < 0.02$ at $T = 4.2$ K for films. On the other hand, the GBS effect becomes the dominant effect at $f_g(T,D,L) \to 1$ when $D/L > 10$ at $T = 4.2$ and 298 K for wires, and when $D/L > 5$ at $T = 298$ K and $D/L > 2.5$ at $T = 4.2$ K for films.

$f_g(T,D,L)$ of polycrystalline films and wires as the function of $T_m^{1/2}$ or R is further investigated with our predicted R from eq 4 at a given $T = 298$ K and $D = L = 50$ nm. Since $l(T,\infty,\infty)$ of metals is basically smaller than D and L, in an approximate way,[5,6] $\Delta\sigma_g(T,L)^{-1}/\sigma(T,\infty,\infty)^{-1} \approx 3l(T,\infty,\infty)R/[2L(1-R)]$, while $\Delta\sigma_s(T,D)^{-1}/\sigma(T,\infty,\infty)^{-1} \approx 3l(T,\infty,\infty)/8D$ for films and $\Delta\sigma_s(T,D)^{-1}/\sigma(T,\infty,\infty)^{-1} \approx 3l(T,\infty,\infty)/4D$ for wires. Using these relations, one has $f_g(T,D,L) = 4R/(1 + 3R)$ for films and $f_g(T,D,L) = 2R/(1+R)$ for wires. As plotted in Figure 5, $f_g(T,D,L)$ functions for both film and wires decrease as $T_m^{1/2}$ or R declines, while $f_g(T,D,L)$ of the former is larger than that of the latter. It is clear that the impact of GBS on suppressing electrical conductance becomes less important for metals with lower T_m.

On the basis of the above discussion, eq 2 with our predicted R can be applied for the materials design in microelectronics with polycrystalline films and wires. For instance, the impact of GBS on $\sigma(T,D,L)$ can be weakened by enlarging L and lowering R. The former can

be carried out by heat treatment[48] and removal of impurities,[14] although this is limited at smaller D.[42,43] The latter can be realized by selecting suitable elements with lower T_m values. Materials such as Al, Ag, Au, and Cu are good candidates apart from their high $\sigma(T,\infty,\infty)$ values.

CONCLUSIONS

A model on R values for metals is newly explored, which is found to be proportional to $T_m^{1/2}$. It enables us to evaluate $\sigma(T,L)$ and thus $\sigma(T,D,L)$ for polycrystalline thin films and wires theoretically, free of adjustable parameters. The impact made by GBS becomes more important upon raising D/L for both films and wires. Compared with wires, the impact of GBS is high for films especially at low T. Moreover, GBS becomes less important for metals with lower melting points. With the theoretical R values, the present $\sigma(T,D,L)$ function is in agreement with available experimental results of polycrystalline Cu, Au, Al, Ag, Pt, Ni, and Nb films and/or wires.

Financial supports by NNSFC (Grant No. 60876074), Program for New Century Excellent Talents in University (NCET-08−0246), National Key Basic Research Development Program (Grant No. 2010CB631001), Young Scholar Projects in Jilin University (200905001), and Program for Changjiang Scholars and Innovative Research Team in University are acknowledged.

Note Added after ASAP Publication: This paper published ASAP on June 17, 2010 with errors in Table 1, an error in the text relating to net variances below eq 2, and additional minor text changes. The correct version was reposted on July 27, 2010.

REFERENCES AND NOTES

1. Ono, T.; Hirose, K. First-Principles Study of Electron-Conduction Properties of Helical Gold Nanowires. *Phys. Rev. Lett.* **2005**, *94*, 206806.
2. Boukai, A.; Xu, K.; Heath, J. R. Size-Dependent Transport and Thermoelectric Properties of Individual Polycrystalline Bismuth Nanowires. *Adv. Mater.* **2006**, *18*, 864–869.
3. Sun, T.; Yao, B.; Warren, A. P.; Barmak, K.; Toney, M. F.; Peale, R. E.; Coffey, K. R. Dominant Role of Grain Boundary Scattering in the Resistivity of Nanometric Cu Films. *Phys. Rev. B* **2009**, *79*, 041402(R).
4. Kitaoka, Y.; Tono, T.; Yoshimoto, S.; Hirahara, T.; Hasegawa, S.; Ohba, T. Direct Detection of Grain Boundary Scattering in Damascene Cu Wires by Nanoscale Four-Point Probe Resistance Measurements. *Appl. Phys. Lett.* **2009**, *95*, 052110.
5. Sondheimer, E. H. The Mean Free Path of Electrons in Metals. *Adv. Phys.* **1952**, *1*, 1–42.
6. Mayadas, A. F.; Shatzkes, M. Electrical-Resistivity Model for Polycrystalline Films: The Case of Arbitrary Reflection at External Surfaces. *Phys. Rev. B* **1970**, *1*, 1382–1389.
7. Au Yeung, T. C.; Chiam, T. C.; Chen, C. K.; Sun, C. Q.; Shangguan, W. Z.; Wong, W. K.; Kam, C. H. Effect of Surface Bond-Order Loss on Electrical Resistivity of Metallic Polycrystalline Thin Films. *Phys. Rev. B* **2005**, *72*, 155417.
8. Dingle, R. B. The Electrical Conductivity of Thin Wires. *Proc. R. Soc., A* **1950**, *201*, 545–560.
9. Soffer, S. B. Statistical Model for the Size Effect in Electrical Conduction. *J. Appl. Phys.* **1967**, *38*, 1710–1715.
10. Reiss, G.; Vancea, J.; Hoffmann, H. Grain-Boundary Resistance in Polycrystalline Metal. *Phys. Rev. Lett.* **1986**, *56*, 2100–2103.
11. Fuchs, K. The Conductivity of Thin Metallic Films According to the Electron Theory of Metals. *Proc. Camb. Phil. Soc.* **1938**, *34*, 100–108.
12. Campbell. D. S. In *The Use of Thin Films in Physical Investigations*; Academic: New York, 196.
13. Larson, D. C.; Boiko, B. T. Electrical Resistivity of Epitaxially Grown Silver Films. *Appl. Phys. Lett.* **1964**, *5*, 155–156.
14. Lim, J. W.; Isshiki, M. Electrical Resistivity of Cu Films Deposited by Ion Beam Deposition: Effects of Grain Size, Impurities, and Morphological Defect. *J. Appl. Phys.* **2006**, *99*, 094909.
15. Lim, J. W.; Mimura, K.; Isshiki, M. Thickness Dependence of Resistivity for Cu Films Deposited by Ion Beam Deposition. *Appl. Surf. Sci.* **2003**, *217*, 95–99.
16. Zhu, Y. F.; Zheng, W. T.; Jiang, Q. Modeling Lattice Expansion and Cohesive Energy of Nanostructured Materials. *Appl. Phys. Lett.* **2009**, *95*, 083110.
17. Parrott, J. E. A New Theory of The Size Effect in Electrical Conduction. *Proc. Phys. Soc.* **1965**, *85*, 1143–1155.
18. Brändli, G.; Cotti, P. Prise en Compte de l'Angle d'Incidence dans la Réflexion des Electrons. *Helv. Phys. Acta* **1965**, *38*, 801–812.
19. Knäbchen, A. Electron Transport through Planar Defects: A New Description of Grain Boundary Scattering. *J. Phys.: Condens. Matter* **1991**, *3*, 6989–6999.
20. Flügge, S.; Marschall, H. In *Rechenmethoden der Quantentheorie*; Springer: Berlin, 1952.
21. Smith, J. R.; Ferrante, J. Grain-Boundary Energies in Metals from Local-Electron-Density Distributions. *Phys. Rev. B* **1986**, *34*, 2239–2245.
22. Gleiter, H. Nanostructured Materials: Basic Concepts and Microstructures. *Acta Mater.* **2000**, *48*, 1–29.
23. Ramaswamy, G.; Raychaudhuri, A. K.; Goswami, J.; Shivashankar, S. A. Large Deviation from Matthiessen's Rule in Chemical Vapor Deposited Copper Films and Its Correlation with Nanostructure. *J. Phys. D* **1997**, *30*, L5–L9.
24. Schneider, M. A.; Wenderoth, M.; Heinrich, A. J.; Rosentreter, M. A.; Ulbrich, R. G. Current Transport through Single Grain Boundaries: A Scanning Tunneling Potentiometry Study. *Appl. Phys. Lett.* **1996**, *69*, 1327–1329.
25. Sambles, J. R.; Elsom, K. C.; Jarvis, D. The Electrical Resistivity of Gold Films. *Phil. Trans. R. Soc.* **1982**, *304*, 365–396.
26. Charton, C.; Fahland, M. Electrical Properties of Ag Films on Polyethylene Terephthalate Deposited by Magnetron Sputtering. *Thin Solid Films* **2004**, *449*, 100–104.
27. Fenn, M.; Akuetey, G.; Donovan, P. E. Electrical Resistivity of Cu and Nb Thin Films. *J. Phys.: Condens. Matter* **1998**, *10*, 1707–1720.
28. Emre Yarimbiyik, A.; Schafftb, H. A.; Allen, R. A.; Vaudinc, M. D.; Zaghloul, M. E. Experimental and Simulation Studies of Resistivity in Nanoscale Copper Films. *Microelectron. Reliab.* **2009**, *49*, 127–134.
29. Qian, L. H.; Lu, Q. H.; Kong, W. J.; Lu, K. Electrical Resistivity of Fully-Relaxed Grain Boundaries in Nanocrystalline Cu. *Scr. Mater.* **2004**, *50*, 1407–1411.
30. Chen, G.; Hui, P.; Pita, K.; Hing, P.; Kong, L. Conductivity Drop Crystallites Redistribution in Gold Film. *Appl. Phys. A: Mater. Sci. Process.* **2005**, *80*, 659–665.
31. Van Attekum, P. M. T. M.; Woerlee, P. H.; Verkade, G. C.; Hoeben, A. A. M. Influence of Grain Boundaries and Surface Debye Temperature on the Electrical Resistance of Thin Gold Films. *Phys. Rev. B* **1984**, *29*, 645–650.
32. Marom, H.; Ritterband, M.; Eizenberg, M. The Contribution of Grain Boundary Scattering *versus* Surface Scattering to the Resistivity of Thin Polycrystalline Films. *Thin Solid Films* **2006**, *510*, 62–67.
33. Marom, H.; Eizenberg, M. The Temperature Dependence of Resistivity in Thin Metal Films. *J. Appl. Phys.* **2004**, *96*, 3319–3323.
34. Artunç, N.; Bilge, M. D.; Utlu, G. The Effects of Grain Boundary Scattering on the Electrical Resistivity of Single-

Layered Silver and Double-Layered Silver/Chromium Thin Films. *Surf. Coat. Technol.* **2007**, *201*, 8377–8381.
35. Smith, J. R. Self-Consistent Many-Electron Theory of Electron Work Functions and Surface Potential Characteristics for Selected Metals. *Phys. Rev.* **1969**, *181*, 522–529.
36. Halasy, S.; Durakiewicz, T. Work Functions of Elements Expressed in Terms of the Fermi Energy and the Density of Free Electrons. *J. Phys.: Condens. Matter* **1998**, *10*, 10815–10826.
37. Jiang, Q.; Lu, H. M. Size Dependent Interface Energy and Its Applications. *Surf. Sci. Rep.* **2008**, *63*, 427–464.
38. Dimoulas, A.; Tsipas, P.; Sotiropoulos, A.; Evangelou, E. K. Fermi-Level Pinning and Charge Neutrality Level in Germanium. *Appl. Phys. Lett.* **2006**, *89*, 252110.
39. Fomenko, V. S. In *Emission Properties of Materials: A Handbook*; Naukova Dumka: Kiev, 1981.
40. Liu, W.; Zheng, W. T.; Jiang, Q. First-Principles Study of the Surface Eenergy and Work Function of III−V Semiconductor Compounds. *Phys. Rev. B* **2007**, *75*, 235322.
41. Lu, H. M.; Wen, Z.; Jiang, Q. Nucleus-Liquid Interfacial Energy of Elements. *Colloids Surf., A* **2006**, *278*, 160–165.
42. Lita, A. E.; Sanchez, J. E. Characterization of Surface Structure in Sputtered Al films: Correlation to Microstructure Evolution. *J. Appl. Phys.* **1999**, *85*, 876–882.
43. Thompson, C. V. Grain-Growth in Thin-Films. *Annu. Rev. Mater. Sci.* **1990**, *20*, 245–268.
44. Marom, H.; Mullin, J.; Eizenberg, M. Size-Dependent Resistivity of Nanometric Copper Wires. *Phys. Rev. B* **2006**, *74*, 045411.
45. Guillaumond, J. F.; Arnaud, L.; Mourier, T.; Fayolle, M.; Pesci, O.; Reimbold, G. Proceedings of the IEEE 2003 International, p132.
46. Wu, W.; Brongersma, S. H.; Van Hove, M.; Maex, K. Influence of Surface and Grain-Boundary Scattering on the Resistivity of Copper in Reduced Dimensions. *Appl. Phys. Lett.* **2004**, *84*, 2838–2840.
47. Casimir, H. B. G. Note on the Conduction of Heat in Crystals. *Physica (Amsterdam)* **1938**, *5*, 495.
48. De Vries, J. W. C. Resistivity of Thin Au Films as a Function of Grain Diameter and Temperature. *J. Phys. F: Met. Phys.* **1987**, *17*, 1945–1952.
49. Skriver, H. L.; Rosengaard, N. M. Surface Energy and Work Function of Elemental Metals. *Phys. Rev. B* **1992**, *46*, 7157–7168.
50. Ashcroft, N. W.; Mermin, N. D. In *Solid State Physics*; Saunders: Philadelphia, 1976.
51. Hauder, M.; Gstöttner, J.; Hansch, W.; Schmitt-Landsiedel, D. Scaling Properties and Electromigration Resistance of Sputtered Ag Metallization Lines. *Appl. Phys. Lett.* **2001**, *78*, 838–840.
52. De Vries, J. W. C. Temperature and Thickness Dependence of the Resistivity of Thin Polycrystalline Aluminium, Nickel, Palladium, Silver and Gold Films. *Thin Solid Films* **1988**, *167*, 25–32.
53. Salvadori, M. C.; Vaz, A. R.; Farias, R. C.; Cattani, M. Electrical Resistivity of Nanostructured Platinum and Gold Thin Films. *Surf. Rev. Lett.* **2004**, *11*, 223–227.
54. Karim, S.; Ensinger, W.; Cornelius, T. W.; Neumann, R. Investigation of Size Effects in the Electrical Resistivity of Single Electrochemically Fabricated Gold Nanowires. *Phys. E* **2008**, *40*, 3173–3178.
55. WebElements. www.webelements.com.
56. Barnat, E. V.; Nagakura, D.; Wang, P. I.; Lu, T. M. Real Time Resistivity Measurements during Sputter Deposition of Ultrathin Copper Films. *J. Appl. Phys.* **2002**, *91*, 1667–1672.
57. Steinhögl, W.; Schindler, G.; Steinlesberger, G.; Traving, M.; Engelhardt, M. Comprehensive Study of the Resistivity of Copper Wires with Lateral Dimensions of 100 nm and Smaller. *J. Appl. Phys.* **2005**, *97*, 023706.
58. Huang, Q. J.; Lilley, C.; M Bode, M.; Divan, R. Surface and Size Effects on the Electrical Properties of Cu Nanowires. *J. Appl. Phys.* **2008**, *104*, 023709.
59. Steinhögl, W.; Schindler, G.; Steinlesberger, G.; Engelhardt, M. Size-Dependent Resistivity of Metallic Wires in the Mesoscopic Range. *Phys. Rev. B* **2002**, *66*, 075414.
60. Aus, M. J.; Szpunar, B.; Erb, U.; El-Sherik, A. M.; Palumbo, G.; Aust, K. T. Electrical Resistivity of Bulk Nanocrystalline Nickel. *J. Appl. Phys.* **1994**, *75*, 3632–3634.
61. Avrekh, M.; Monteiro, O.; R. Brown, I. G. Electrical Resistivity of Vacuum-arc-Deposited Platinum Thin Films. *Appl. Surf. Sci.* **2000**, *158*, 217–222.
62. Larson, D. C.; Boiko, B. T. Electrical Resisty of Thin Epitaxially Grown Silver Films. *Appl. Phys. Lett.* **1964**, *5*, 155–156.
63. Ou, M. N.; Yang, T. J.; Harutyunyan, S. R.; Chen, Y. Y.; Chen, C. D.; Lai, S. J. Electrical and Thermal Transport in Single Nickel Nanowire. *Appl. Phys. Lett.* **2008**, *92*, 063101.
64. Fischer, G.; Hoffman, H. Oscillations of the Electrical Conductivity with Film Thickness in Very Thin Platinum Films. *Solid State Commun.* **1980**, *35*, 793–796.
65. Bandyopadhyay, S. K.; Pal, A. K. The Effect of Grain Boundary Scattering on the Electron Transport of Aluminium Films. *J. Phys. D: Appl. Phys.* **1979**, *12*, 953–959.
66. Tochitskii, E. I.; Relyavskii, N. M. Grain-Boundary Electron Scattering Effect on Metal Film Resistivity. *Phys. Status Solidi A* **1980**, *61*, K21–K24.
67. Mannan, K. M.; Karim, K. R. Grain Boundary Contribution to the Electrical Conductivity of Polycrystalline Cu Films. *J. Phys. F: Met. Phys.* **1975**, *5*, 1687–1693.
68. Zhang, W.; Brongersma, S. H.; Clarysse, T.; Terzieva, V.; Rosseel, E.; Vandervorst, W.; Maex, K. Surface and Grain Boundary Scattering Studied in Beveled Polycrystalline Thin Copper Films. *J. Vac. Sci. Technol., B* **2004**, *22*, 1830.
69. Artunç, N.; Öztürk, Z. Z. Influence of Grain-Boundary and Surface Scattering on the Electrical Resistivity of Single-Layered Thin Copper Films. *J. Phys.: Condens. Matter* **1993**, *5*, 559.
70. Kuan, T. S.; Inoki, C. K.; Oehrlein, G. S.; Rose, K.; Zhao, Y. P.; Wang, G. C.; Rossnagel, S. M.; Cabral, C. Fabrication and Performance Limits of Sub-0.1 mm Cu Interconnects. In *Material Research Society Symposium Proceedings*; Materials Research Society: Warrendale, PA, 2000; pp D7.1.1.
71. Zhang, Q. G.; Cao, B. Y.; Zhang, X.; Fujii, M.; Takahashi, K. Size Effects on the Thermal Conductivity of Polycrystalline Platinum Nanofilms. *J. Phys.: Condens. Matter* **2006**, *18*, 7937–7950.
72. Botcharova, E.; Freudenberger, J.; Schultz, L. Mechanical and Electrical Properties of Mechanically Alloyed Nanocrystalline Cu−Nb Alloys. *Acta Mater.* **2006**, *54*, 3333–3341.
73. Ederth, J.; Kiss, L. B.; Niklasson, G. A.; Granqvist, C. G.; Olsson, E. Temperature Dependence of the Electrical Resistivity in Nanocrystalline Gold Films Made by Advanced Gas Deposition. *Mater. Res. Soc. Symp. Proc.* **2000**, *581*, 541–546.
74. Cheng, S.; Ma, E.; Wang, Y. M.; Kecskes, L. J.; Youssef, K. M.; Koch, C. C.; Trociewitz, U. P.; Han, K. Tensile Properties of in situ Consolidated Nanocrystalline Cu. *Acta Mater.* **2005**, *53*, 1521–1533.
75. Kita, E.; Shiozawa, K.; Sasaki, Y.; Iwamoto, Y.; Tasake, A. Ni and NiFe Nanocrystalline Films Prepared with Gas-Deposition Method. *IEEE Trans. Magn.* **1996**, *32*, 4487–4489.
76. Liu, H. D.; Zhao, Y. P.; Ramanath, G.; Murarka, S. P.; Wang, G. C. Thickness Dependent Electrical Resistivity of Ultrathin (< 40 nm) Cu Films. *Thin Solid Films* **2001**, *384*, 151–156.
77. Kim, C. U.; Park, J. Y.; Michael, N.; Gillespie, P.; Augur, R. Study of Electron-Scattering Mechanism in Nanoscale Cu Interconnects. *J. Electron. Mater.* **2003**, *32*, 982.
78. Shimada, M.; Moriyama, M.; Ito, K.; Tsukimoto, S.; Murakami, M. Electrical Resistivity of Polycrystalline Cu Interconnects with Nanoscale Linewidth. *J. Vac. Sci. Technol. B* **2006**, *24*, 190–194.
79. Maîtrejean, S.; Gers, R.; Mourier, T.; Toffoli, A.; Passemard, G. Experimental Measurements of Electron Scattering Parameters in Cu Narrow Lines. *Microelectro. Engin.* **2006**, *83*, 2396–2401.
80. Durkan, C.; Welland, M. E. Size Effects in the Electrical Resistivity of Polycrystalline Nanowires. *Phys. Rev. B* **2000**, *61*, 14215–14218.